Computational and Structural Biotechnology Journal 27 (2025) 278–286

Contents lists available at ScienceDirect

Computational and Structural Biotechnology Journal

journal homepage: www.elsevier.com/locate/csbj

Research article

Artificial intelligence-enhanced electrocardiography improves the detection of coronary artery disease

Chi-Hsiao Yeh [a,b,c], Tsung-Hsien Tsai [d], Chun-Hung Chen [d], Yi-Ju Chou [e], Chun-Tai Mao [b,c,f], Tzu-Pei Su [c,g], Ning-I Yang [b,c,f], Chi-Chun Lai [b,c,h], Chien-Tzung Chen [c,i,*], Huey-Kang Sytwu [j,k,*], Ting-Fen Tsai [e,l,m,*]

[a] Department of Thoracic and Cardiovascular Surgery, Chang Gung Memorial Hospital, Linkou, Taoyuan 333, Taiwan
[b] Community Medicine Research Center, Chang Gung Memorial Hospital, Keelung 204, Taiwan
[c] College of Medicine, Chang Gung University, Taoyuan 333, Taiwan
[d] Advanced Tech BU, Acer Inc., New Taipei City 221, Taiwan
[e] Institute of Molecular and Genomic Medicine, National Health Research Institutes, Miaoli 350, Taiwan
[f] Division of Cardiology, Department of Internal Medicine, Chang Gung Memorial Hospital, Keelung 204, Taiwan
[g] Department of Nuclear Medicine, Chang Gung Memorial Hospital, Keelung 204, Taiwan
[h] Department of Ophthalmology, Chang Gung Memorial Hospital, Keelung 204, Taiwan
[i] Department of Plastic & Reconstructive Surgery, Chang Gung Memorial Hospital, Linkou, Taoyuan 333, Taiwan
[j] National Institute of Infectious Diseases and Vaccinology, National Health Research Institutes, Miaoli 350, Taiwan
[k] Department & Graduate Institute of Microbiology and Immunology, National Defense Medical Center, Taipei 114, Taiwan
[l] Department of Life Sciences and Institute of Genome Sciences, National Yang Ming Chiao Tung University, Taipei 112, Taiwan
[m] Center for Healthy Longevity and Aging Sciences, National Yang Ming Chiao Tung University, Taipei 112, Taiwan

ARTICLE INFO

Keywords:
Electrocardiograms
Coronary artery disease
Artificial intelligence

ABSTRACT

An AI-assisted algorithm has been developed to improve the detection of significant coronary artery disease (CAD) in high-risk individuals who have normal electrocardiograms (ECGs). This retrospective study analyzed ECGs from patients aged ≥ 18 years who were undergoing coronary angiography to obtain a clinical diagnosis at Chang Gung Memorial Hospital in Taiwan. Utilizing 12-lead ECG datasets, the algorithm integrated features like time intervals, amplitudes, and slope between peaks, a total of 561 features, with the XGBoost model yielding the best performance. The AI-enhanced ECG algorithm demonstrated high sensitivity (0.82–0.84) when detecting CAD in patients with normal ECGs and gave remarkably high prediction rates among those with abnormal ECGs, both with and without ischemia (92 %-95 % and 80 %-83 %, respectively). Notably, the algorithm's top features, mostly related to slope and amplitude differences, are challenging for clinicians to discern manually. Additionally, the study highlights significant sex differences regarding feature prediction and ranking. Comparatively, the AI-enhanced ECG's detection capability matched that of myocardial perfusion scintigraphy, which is a costly nuclear medicine test, and offers a more accessible alternative for identifying significant CAD, especially among patients with atypical ECG readings.

1. Introduction

Electrocardiograms (ECG) provide a window that allows the detection of cardiac arrhythmia [1] and dysfunction [2–4]; they can also provide valuable diagnostic clues in relation to electrolyte derangement [5] and toxic drug reactions [6]. Currently, computer-generated interpretations that are based on predefined rules and manual pattern/-feature recognition algorithms have been used for a number of years [7]. However, these interpretations, even when re-confirmed by an experienced cardiologist, are unable to completely capture the complexity and nuances of an ECG.

Coronary artery disease (CAD) is one of the most common heart diseases. It is caused by plaque buildup in the major blood vessels that supply the heart, namely the coronary arteries. Detection of significant CAD is the most important goal when evaluating patients with symptoms that are possibly due to coronary artery ischemia [8]. Among

* Correspondence to: No 155, Section 2, Li-Nong St, Beitou Dist., Taipei 112304, Taiwan.
E-mail addresses: ctchenap@cgmh.org.tw (C.-T. Chen), sytwu@nhri.edu.tw (H.-K. Sytwu), tftsai@nycu.edu.tw (T.-F. Tsai).

https://doi.org/10.1016/j.csbj.2024.12.032
Received 11 October 2024; Received in revised form 23 December 2024; Accepted 26 December 2024
Available online 27 December 2024

patients who are "ruled in" for myocardial infarction (MI) during admission to monitored beds, only approximately 30 % of patients with CAD are able to be detected by ECG. Among patients with left main coronary artery stenosis, about 75 % of the patients have a normal pattern for their resting ECG [9]. Even among patients with acute MI (within 2 hours of chest pain), the ECG is found to be completely normal 15 % of the time. The insensitivity of ECG when detecting MI has been shown across many different clinical studies [10,11]. Thus, currently, a normal resting ECG is no guarantee that CAD is absent. Moreover, even when myocardial ischemia is clearly present, a proportion of patients with severe CAD still have no overt changes in ECG [8]. The diagnostic sensitivity of ECG in terms of 30-day major cardiac events among patients with acute chest pain is between 12.6 % and 50 % [12]. Since ECG is the most common painless test for the quick detection of heart problems, increasing the sensitivity of resting ECG analysis in order to identify patients with CAD in both symptomatic and asymptomatic patients is an unmet need clinically.

Artificial intelligence (AI) algorithms have been successfully applied to identify high-risk patients who have a likelihood of having certain cardiac disorders based on a conventional ECG; examples include contractile dysfunction and atrial fibrillation [3,6,13–17]. However, the application of AI-algorithms for the detection of CAD has been explored to a lessor extent. We have found only one report that used convolutional neural networks for image analysis in order to detect significant CAD (>70 % stenosis) [18]. In this study, we develop an AI-algorithm to improve the detection of CAD among high-risk subjects with normal ECGs. Furthermore, we apply our AI-algorithm to clinically diagnosed CAD patients who have abnormal ECGs in order to evaluate the reliability of this AI-algorithm and to aid healthcare professionals to obtain a precise diagnosis. Moreover, the sex and the age of patients is known to have a tremendous influence on the patterns and interpretation of ECGs [19–22], and this has been taken into consideration during the development of the AI-algorithm in an attempt to enhance the sensitivity and the accuracy of ECG detection of CAD.

2. Methods and materials

2.1. Study design

The present study was approved by the Institutional Review Board of Chang Gung Medical Foundation (IRB No: 201800724B0, 202001605B0C101, and 202000077B0A3). The 12 Lead 10-second ECGs included in groups 1–3 had to have been collected either no more than one month before coronary angiography (CAG), or after CAG (Fig. 1A). Those subjects in group 0 (only normal ECGs) were recruited as having ages between 18 and 39 years [23]. The definition of a normal ECG (group 0 and 1) is defined as nothing but a normal sinus rhythm recorded in the ECG report. ECGs with any other comments besides sinus rhythm on the report were categorized as abnormal ECGs. Patients with abnormal ECGs without and with ischemic descriptions were classified into groups 2 and 3, respectively. Ischemic descriptions were defined as any of the following in the ECG reports: MI, infarct, infarction, ischemia,

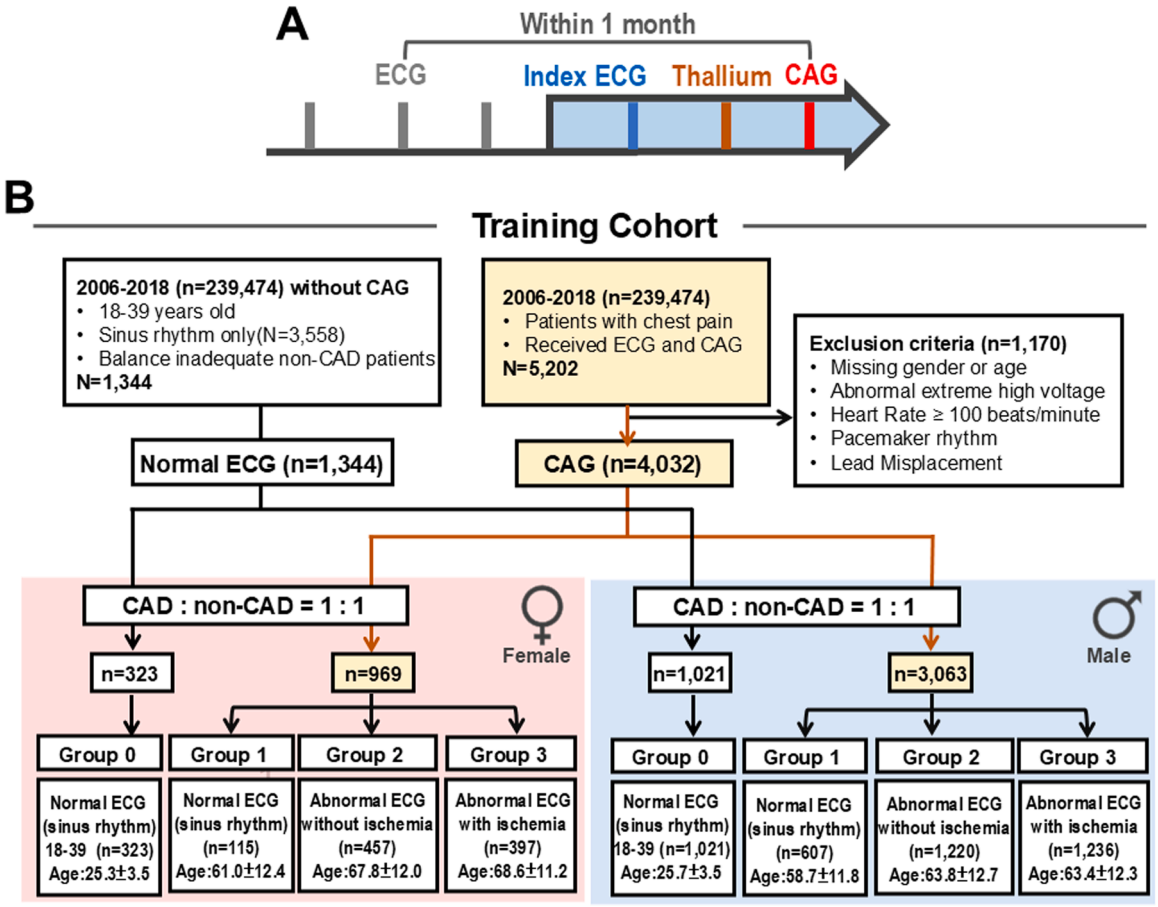

Fig. 1. Patient flow diagram and examples that support the performance of the AI-enhanced ECG approach. (A) ECGs are included in this retrospective study under the following criteria, that they are the latest ECG records and were obtained no more than 1 month before a patient received coronary angiography (CAG). (B) The training cohort is composed of four groups. Group 0: normal ECG (sinus rhythm only) obtained from subjects at a young age (18–39 years old); this group is to balance the dominant number of CAD patients. Group 1: normal ECG with a description of sinus rhythm only. Group 2: abnormal ECG without an ischemic description. Group 3: abnormal ECG with an ischemic description (ischemic descriptions include the following key words: MI, infarct, infarction, ischemia and subendocardial injury).

and subendocardial injury. All ECG and CAG reports were evaluated and labeled by two experienced cardiologists.

2.2. Training cohort

Subjects were collected between January 2006 and December 2018. A total of 239,474 ECGs and their medical records were obtained from Chang Gung Memorial Hospital, which is located in Keelung City, Taiwan, and these were retrospectively reviewed (Table 1 and Fig. 1B). In total 5202 patients received both ECG and CAG examinations; these patients are our main research subjects. Of these patients, 1170 ECGs were excluded due to tachycardia (≥100 bpm), pacemaker rhythm, lead misplacement, or extremely high voltage (>10 mV). To balance the inadequate number of non-CAD subjects, another 1344 normal ECGs, which were randomly selected from 3588 non-CAD subjects, who ages ranged from 18 to 39 years old, were used; these were included as group 0. To minimize training bias, we adjusted the sample ratio of CAD to non-CAD ECGs to be 1:1 in the training cohort.

2.3. Validation cohort

Subjects were collected between January 2018 and December 2018 from a different Chang Gung Memorial Hospital located in Taoyuan City, Taiwan. A total of 2893 patients, who received ECG and CAG examinations, were obtained from Chang Gung Memorial Hospital, Linkou, and these were then retrospectively reviewed (Table 1 and Fig. S1). Of these patients, 265 ECGs were excluded following the same criteria as the training cohort. To test the reliability of our AI-algorithm, another 4535 normal ECGs were obtained from a group of young subjects aged between 18 and 39 years old and these were also included as normal controls; these were selected from a total of 99,797 ECGs carried out over the same period.

Expanded methods are provided in the Online Supplementary file

3. Results

3.1. Clinical characteristics of the subjects

The baseline characteristics of the training and validation cohorts are presented in Table 1. In the training cohort (n = 5376), the subjects were divided into four groups. Firstly, Group 0 (n = 1344), who had a normal sinus rhythm and were young (age 25.6 ± 3.5 years old); this group was used to balance the dominant number of CAD patients. Secondly, Group 1, which consisted of individuals with a normal sinus rhythm (n = 722) based on their CAG results; these subjects were divided into a CAD subgroup (n = 356; 49.3 %; 61.1 ± 11.2 years old) and a non-CAD group (n = 366; 50.7 %; 57.3 ± 12.2 years old). Thirdly, Group 2, which consisted of subjects with an abnormal ECG without ischemia (n = 1677); these were divided into a CAD subgroup (n = 1026; 61.2 %; 67.0 ± 12.0 years old) and a non-CAD subgroup (n = 651; 38.8 %; 61.6 ± 12.9 years old). Finally, Group 3, who had abnormal ECGs with ischemia (1633); these were subdivided into individuals with CAD (n = 1306; 80.0 %; 65.2 ± 11.9 years old) and

Table 1
Characteristics of patients.

Training cohort (n = 5376)										
Conventional ECG (n)	Sinus rhythm only				Abnormal ECG without ischemic description (1677)			Abnormal ECG with ischemic description (1633)		
	(1344)	(722)								
Group	0	1			2			3		
CAG result	N/A	CAD (-)	CAD (+)		CAD (-)	CAD (+)		CAD (-)	CAD (+)	
n (%)	1344	366 (50.7)	356 (49.3)		651 (38.8)	1026 (61.2)		327 (20.0)	1306 (80.0)	
Age (y)	25.6 ± 3.5	57.3 ± 12.2	61.1 ± 11.2	< 0.0001	61.6 ± 12.9	67.0 ± 12.0	0.0098	62.3 ± 13.4	65.2 ± 11.9	0.0001
Male sex, n (%)	1021 (76.0)	307 (42.5)	300 (41.6)	0.02	479 (28.6)	741 (44.2)	ns	235 (14.4)	1001 (61.3)	ns
BMI	23.8 ± 3.3	26.6 ± 4.3	25.8 ± 3.9	0.009	26.1 ± 4.8	25.2 ± 4.2	< 0.0001	25.6 ± 5.0	25.2 ± 4.2	ns
Diabetes, n (%)	10 (0.7)	105 (14.5)	162 (22.4)	< 0.0001	188 (11.2)	461 (27.5)	< 0.0001	86 (5.3)	579 (35.5)	< 0.0001
Hypertension, n (%)	15 (1.1)	187 (25.9)	251 (34.8)	< 0.0001	376 (22.4)	751 (44.8)	< 0.0001	176 (10.8)	830 (50.8)	0.019
Renal disease, n (%)	2 (0.1)	34 (4.7)	66 (9.1)	< 0.0001	134 (8.0)	347 (20.7)	< 0.0001	64 (3.9)	372 (22.8)	< 0.0001
MI, n (%)	-	-	307 (42.5)	< 0.0001	-	799 (47.6)	< 0.0001	-	967 (59.2)	< 0.0001
Cath diagnosis										
LM≥ 50 %, n (%)	-	0	30 (4.2)	< 0.0001	0	141 (8.4)	< 0.0001	0	171 (10.5)	< 0.0001
LAD≥ 70 %, n (%)	-	0	201 (27.8)	< 0.0001	0	596 (35.5)	< 0.0001	0	909 (55.7)	< 0.0001
LCX≥ 70 %, n (%)	-	0	139 (19.3)	< 0.0001	0	504 (30.1)	< 0.0001	0	630 (38.6)	< 0.0001
RCA≥ 70 %, n (%)	-	0	153 (21.2)	< 0.0001	0	564 (33.6)	< 0.0001	0	766 (46.9)	< 0.0001
Validation cohort (n = 7163)										
Conventional ECG (n)	Sinus rhythm only				Abnormal ECG without ischemic description (1103)			Abnormal ECG with ischemic description (1148)		
	(4535)	(377)								
Group	0	1			2			3		
CAG result	N/A	CAD (-)	CAD (+)		CAD (-)	CAD (+)		CAD (-)	CAD (+)	
n (%)	4535	193 (51.2)	184 (48.8)		521 (47.2)	582 (52.8)		345 (30.1)	803 (69.9)	
Age (y)	31.4 ± 6.2	58.6 ± 12.0	61.7 ± 10.7	0.0086	62.2 ± 13.3	65.8 ± 12.1	< 0.0001	61.6 ± 14.6	64.5 ± 12.8	0.0008
Male sex, n (%)	1903 (42.0)	138 (36.6)	153 (40.6)	0.007	327 (29.6)	442 (40.1)	< 0.0001	220 (19.2)	627 (54.6)	< 0.0001
BMI	23.9 ± 4.0	26.3 ± 4.4	27.2 ± 4.1	0.04	26.0 ± 4.7	26.0 ± 3.7	ns	25.8 ± 4.4	25.9 ± 4.4	ns
Diabetes, n (%)	36 (0.8)	50 (13.3)	87 (23.1)	< 0.0001	119 (10.8)	312 (28.3)	< 0.0001	55 (4.8)	415 (36.1)	< 0.0001
Hypertension, n (%)	54 (1.2)	102 (27.1)	132 (35.0)	0.0002	260 (23.6)	515 (46.7)	< 0.0001	128 (11.1)	603 (52.5)	< 0.0001
Renal disease, n (%)	5 (0.1)	20 (5.3)	35 (9.3)	0.017	101 (9.2)	234 (21.2)	< 0.0001	40 (3.5)	268 (23.3)	< 0.0001
MI, n (%)	-	-	158 (41.9)	< 0.0001	-	537 (48.7)	< 0.0001	-	657 (57.2)	< 0.0001
Cath diagnosis										
LM≥ 50 %, n (%)	-	0	13 (3.4)	< 0.0001	0	59 (5.3)	< 0.0001	0	81 (7.1)	< 0.0001
LAD≥ 70 %, n (%)	-	0	124 (32.9)	< 0.0001	0	333 (30.2)	< 0.0001	0	526 (45.8)	< 0.0001
LCX≥ 70 %, n (%)	-	0	91 (24.1)	< 0.0001	0	261 (23.7)	< 0.0001	0	350 (30.5)	< 0.0001
RCA≥ 70 %, n (%)	-	0	103 (27.3)	< 0.0001	0	296 (26.8)	< 0.0001	0	451 (39.3)	< 0.0001

CAG, coronary angiography; BMI, body mass index; MI, myocardial infarction; LM, left main coronary artery; LAD, left anterior descending coronary artery; LCX, left circumflex coronary artery; RCA, right coronary artery.

individuals without non-CAD (n = 327; 20.0 %; 62.3 ± 13.4 years old) (Table 1 and Fig. 1A-B). In the validation cohort (n = 7163), the subjects were collected from the same hospital that is located in a different city. In both of the above cohorts, patients with CAD in groups 1–3 were found to have more comorbidities, including diabetes mellitus (DM), hypertension, renal insufficiency, and MI, compared with those patients without CAD in the same group. Furthermore and notably, the left anterior descending (LAD) coronary artery is the most common lesion site among the CAD patients (Table 1 and Fig. S1).

3.2. *The use of the AI-algorithm enhances the sensitivity of an ECG when detecting CAD*

To enhance the sensitivity of the detection of CAD among subjects with normal ECGs, we trained our AI-algorithm using the training cohort (Fig. 1A-B) and the validation cohort (Fig. S1). The labeling, pre-processing and feature engineering of the ECGs are described in methods section (Suppl. Fig. 2). Most of the time windows between the ECG examinations and the CAG examinations were less than 7 days (Suppl. Fig. 3).

The flow chart of the ML is briefly summarized in Fig. 2A. Notably, in

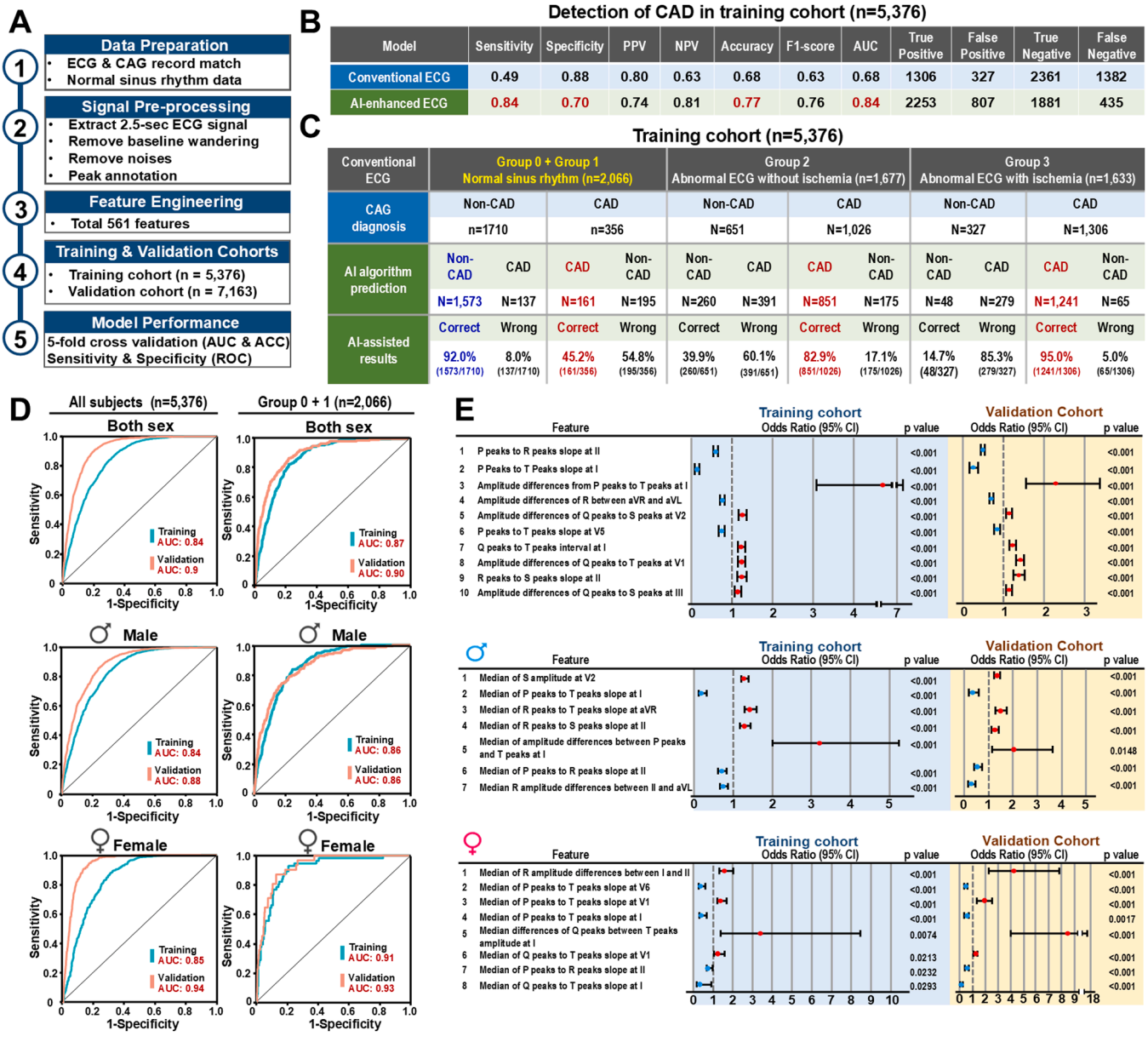

Fig. 2. Performance of the AI-enhanced ECG when detecting CAD. (A) Flow chart of ML, including data preparation, signal pre-processing and feature engineering using training and validation cohorts. The network accepts raw ECG xml data as an input and outputs a prediction of CAD probability. Performance of the AI-algorithm is carried out by 5-fold cross validation and evaluated using the results of the area under curve (AUC) under the Receiver Operator Characteristic Curve (ROC) approach, accuracy rate (ACC), sensitivity, specificity, positive (PPV) and negative (NPV) predictive values. (B) The AI-algorithm enhances the performance of the ECGs compared with conventional ECGs in the training cohort. F1 score is calculated as the harmonic mean of the precision and recall scores. (C) The prediction rates of the AI-enhanced ECG algorithm in subjects with normal sinus rhythm (Groups 0 + 1), Group 2 and Group 3 from the training cohort. (D) ROC curves calculated for the detection of CAD in all subjects and subjects with a normal sinus rhythm (Group 0 + Group 1). Green curve is the training cohort, while orange curve is the validation cohort. The AUC values for the training and validation cohorts are also shown. (E) Adjusted odds ratios (OR) of features associated with the occurrence of CAD in subjects with normal ECGs. The Wald test was used to construct 95 % confidence intervals (CIs) and test the significance of the adjusted ORs of the risk factors. The error bars represent the lower boundary and the upper boundary of the adjusted OR of 95 % CI.

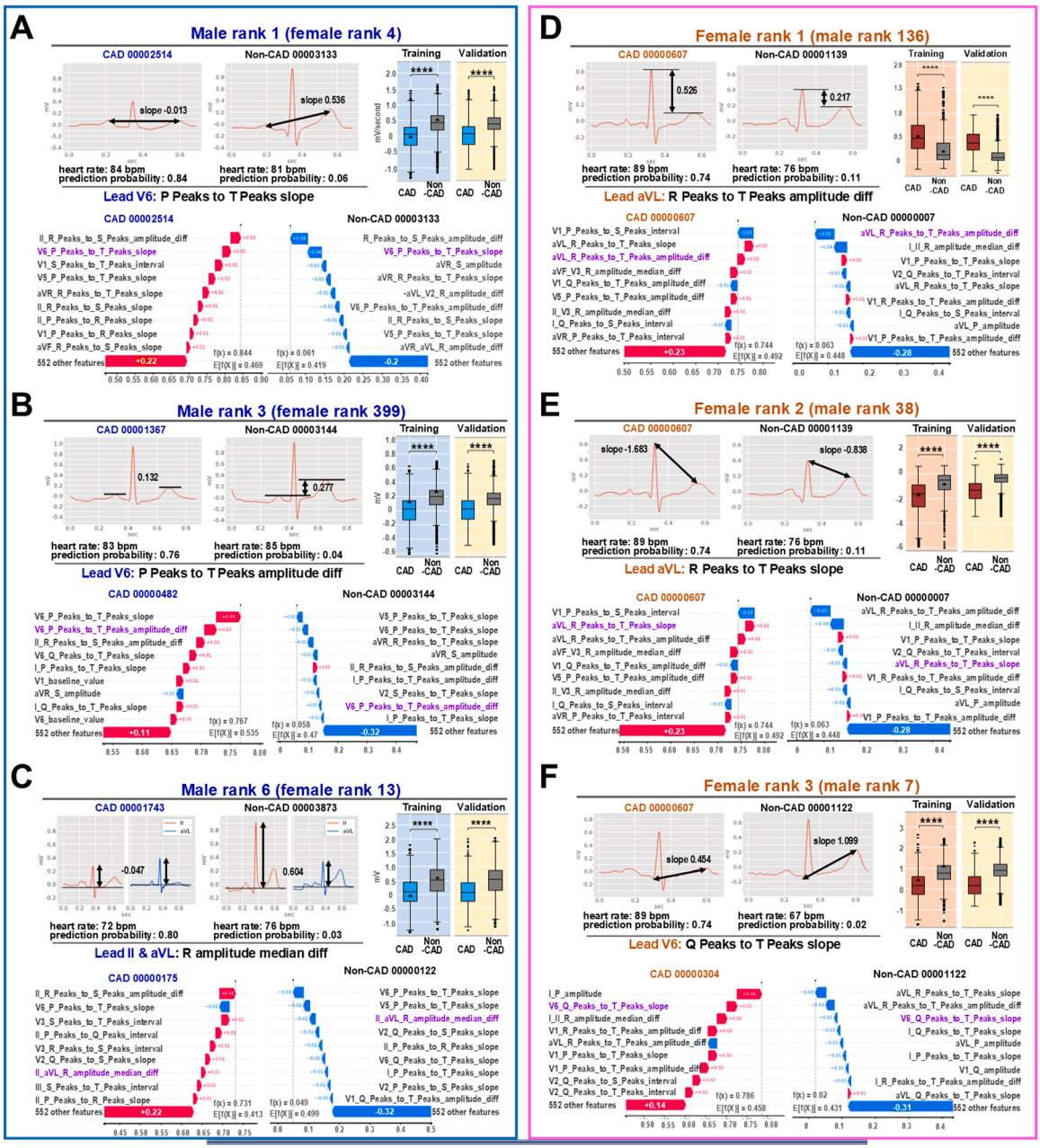

Fig. 3. Sex differences, examples of the top ranked ECG features and the composition of the probability of CAD prediction in CAD and non-CAD subjects. (A-C) Examples presented are the three top ranked features (rank #1, #3 and #6) of males. (D-F) Examples presented are the three top ranked features (rank #1, #2 and #3) of females. Box plots of the feature with statistically significant differences between CAD and non-CAD patients are shown. The probability of CAD prediction is calculated by adding the Shapley additive explanations (SHAP) values of the top nine features and the remaining 552 features. A positive SHAP value (red bar) means a contribution to the probability of CAD and a negative SHAP value (blue bar) means the opposite. Each individual has a personal list of feature ranked by SHAP framework. * ** *$p < 0.0001$.

the training cohort (all subjects; n = 5376), the AI-enhanced ECG algorithm has a high sensitivity when identifying CAD, namely 0.84, when compared with the sensitivity of a conventional ECG, namely 0.49. In addition, the AI-algorithm also has a good performance, with an accuracy rate of 0.77 and an AUC of 0.84, when detecting potential CAD (Fig. 2B). Remarkably, in the validation cohort (n = 7163; CAD: Non-CAD = 1569: 5594), the performance is even better giving the following results: sensitivity (0.82), accuracy rate (0.85) and AUC (0.91) (Suppl. Figs. 4A and S5).

Among the subjects with a normal sinus rhythm in the training cohort (Groups 0 + 1; n = 2066), there are 356 patients with CAD based on the CAG diagnosis. Interestingly, our AI-algorithm was able to identify 45.2 % of these subjects (161/356) (Fig. 2C). Consistently, in the subjects with a normal sinus rhythm in the validation cohort (Groups 0 + 1; n = 4912), about 47.3 % (87/184) of the CAD patients were able to be identified (Fig. S4B). The overall performance of the AI-algorithm when detecting CAD in subjects with a normal sinus rhythm is shown in Fig. S4C-D. Regarding the performance of the AI-algorithm when used on Group 2 (abnormal ECG without ischemia), about 82.9 % and 80.2 % of CAD patients can be identified in the training and validation cohorts, respectively; while in Group 3 (abnormal ECG with ischemia), about 95.0 % and 91.9 % of CAD patients can be identified in the training and validation cohorts, respectively (Fig. 2C; Fig. S4B).

Furthermore, when AUC, which plots the sensitivity (true positive

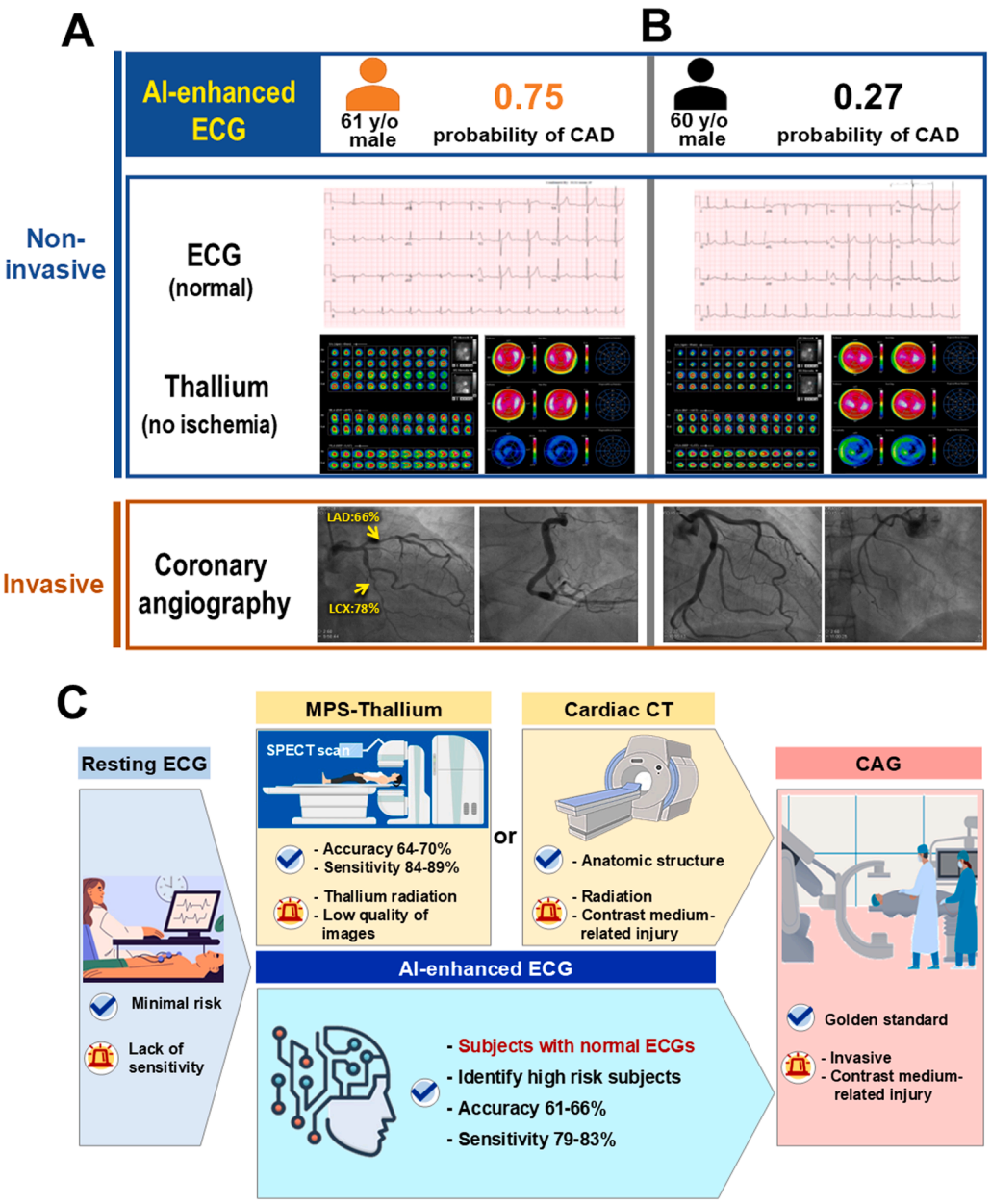

Fig. 4. Comparison of Diagnostic Modalities for Coronary Artery Disease. (A) An example of a 61-year-old male CAD patient who has a normal ECG and a negative result by Thallium scanning. However, his CAG result revealed that he has a significant infarction in the LAD and LCX coronary arteries. Interestingly, the AI-enhanced ECG algorithm predicts the probability of CAD to be 0.75 for this subject. (B) Another example of a 60-year-old male non-CAD patient, who has a normal ECG and a negative Thallium scan; he has normal coronary arteries as revealed by CAG. Notably, the AI-enhanced ECG algorithm predicts a low probability of CAD, namely 0.27, for this subject. (C) Our AI-enhanced ECG algorithm should be able to provide an alternative approach when identifying high-risk subjects with potential CAD. For patients with chest pain, initial examination by resting 12-lead ECG, followed by nuclear medicine examination, namely myocardial perfusion scintigraphy (MPS)-Thallium scanning or cardiac computerized tomography (CT), then invasive coronary angiography (CAG), is recommended currently. Our AI-enhanced ECG algorithm has a performance comparable with MPS-Thallium scanning and thus it may serve as an alternative screening method.

rate; y coordinate) versus its 1-specificity (false positive rate; x coordinate), was used to evaluate the overall performance of the AI-enhanced ECG algorithm. The results for the AUC of the 5-fold cross validation for all of the subjects and subjects with a normal sinus rhythm (Groups 0 + 1) in the training as well as validation cohorts are presented in Fig. 2D.

3.3. A panel of novel ECG features that identifies high-risk subjects

Our model is built using XGBoost, which gave the best performance using ML. The XGBoost model is a tree-based model, and the importance of a feature is ranked according to the improvement in accuracy brought about by a feature to the branches within it. Hence for each feature, it is possible to calculate the improvement (information gain) for the tree branches. A total of 561 ECG features were used to predict the probability of CAD (Fig. S2C). In addition, we conduct multifactorial analysis by logistic regression to elucidate the relationships between the features and the occurrence of CAD in the subjects with normal ECGs (Fig. 2E). When combining males and females, there are ten features that have statistically significance. Among these ten features, it was found that an increase in the adjusted odds ratios (OR) is present for the occurrence of CAD in relation to six of these features. Conversely, there are four features that appear to be associated with a lower risk of CAD. Furthermore, in males, there are seven ECG features that have statistically

significance. Among these seven features, six features are recorded from the limb leads (I, II, aVR and aVL), and only one feature is recorded from the chest lead, namely V2. By way of contrast, [n females, there are eight features that have statistically significance. Among these eight features, five features are recorded from the limb leads (I and II), and three features are from the chest leads (V1 and V6).

Intriguingly, all of these AI-selected features have never been mentioned in the current diagnostic criteria for MI. Furthermore, most of these top ranked features are associated with the slope and amplitude difference between peaks, suggesting that these features may play key roles in detecting ECG abnormalities and there is an implication that they are related to the stenotic condition of the coronary arteries.

3.4. Sex difference and the ranking of ECG features

Growing evidence has revealed that there are substantial differences in the incidence of clinical presentation of CAD and the mortality from CAD between males and females [24]. Consistently, these sex differences can also be reproducibly observed in our cohorts. For example, the average ages of the female patients with abnormal ECGs in Group 2 and Group 3 are significantly higher than those of the male patients (Fig. 1B). Additionally, the features selected for the odds ratio analyses are different for males and females (Fig. 2E). Accordingly, we have ranked the features for all of the subjects combining both sexes, as well those for the males and females separately (Table S1). Remarkably, the order of the features and the items making up the top 15 features for the males and females are very different. In order to explore the ECG features associated with the difference in sex, we show in Fig. 3 several examples from CAD and non-CAD subjects.

In males, the rank #1 feature is the median slope of the P to T peaks from the lead V6. Notably, male CAD patients have significantly lower values for the median slope compared with non-CAD individuals in both cohorts. For example, in CAD patient 0002514, a negative median slope (-0.013) of this feature contributes a + 0.02 possibility of CAD. Furthermore, in this patient, the top nine features increase the possibility of CAD from + 0.70 to + 0.844, while the remaining 552 features altogether contribute only + 0.22 to the possibility of CAD. On the other hand, in non-CAD subject 00003133, a positive median slope (0.536) of this feature decreases the possibility of CAD by −0.04. Interestingly, in this subject, the top nine features decrease the possibility of CAD from 0.219 to 0.061. On the other hand, the remaining 552 features together only contribute a −0.2 to the possibility of CAD (Fig. 3A). In addition, among males, the rank #3 feature is the median value of the P peaks to T peak amplitude difference at lead V6; a significantly lower value for this is observed in CAD patients. Furthermore, the rank #6 feature is the median value of the R amplitude difference between leads II and aVL and again there is a significantly lower value observed in CAD patients. Examples of CAD and non-CAD predictions using these two features are also provided (Fig. 3B-C).

In females, the rank #1 feature of the AI algorithm is the median value of the amplitude difference between the R and T peaks for lead aVL. Remarkably, CAD patients have a significantly higher value of this feature in both cohorts. Moreover, among females, the rank #2 feature is the median slope of the R peaks to T peaks for lead aVL and this has a significantly lower value among female CAD patients. Furthermore, the rank #3 feature is the median slope of the Q peaks to T peaks for lead V6 and this has a significantly lower value among female CAD patients. Examples of the CAD and non-CAD predictions using these features are provided in Fig. 3D-F.

Overall, the SHAP value of each feature shows a preference toward either a higher risk or a lower risk for the occurrence of CAD. On the addition of the SHAP values of all 561 features, this value reflects the final prediction score of the model. Furthermore, the ranking of features represents the most frequently appearing features that are of higher importance to the prediction; accordingly, it also represents the importance of features for the model itself, but not specifically for a given individual. At the personal level, each individual has a personal feature ranking list that is calculated via the SHAP framework. Knowledge of a patient's feature ranking list should be able to help clinicians pinpoint the characteristics of an individual's abnormal ECG patterns and thereby help the doctor to select appropriate medication and the best treatment options.

3.5. Comparison between AI-enhanced ECGs and Thallium scans

Myocardial perfusion scintigraphy (MPS) with Thallium 201, which is a nuclear medicine test, is one of the most important and common non-invasive cardiac imaging methods. It has been recommended as a gatekeeper before the implementation of an invasive CAG procedure [25]. To test the utility of our AI-algorithm, we compare the performance of our AI-enhanced ECG algorithm with MPS-Thallium scanning and conventional ECGs (Table 2). Subjects in the training (n = 1049) and validation (n = 528) cohorts used in this comparison have medical records for MPS-Thallium scans and for conventional ECGs. Remarkably, the sensitivity of detection of CAD is significantly increased by both the AI-enhanced ECG algorithm, namely to 0.79 and 0.83 in the training and validation cohorts, respectively, and by MPS-Thallium scanning, namely to 0.84 and 0.89 in the training and validation cohorts, respectively. Moreover, the accuracy and AUC are also much higher for AI-enhanced ECG algorithms and MPS-Thallium scans compared with conventional ECGs. Overall, the performance of the AI-enhanced ECG algorithm and MPS-Thallium scanning are similar and comparable in terms of sensitivity, accuracy and AUC (Table 2). Additionally, compared with conventional ECG, the advantage of using AI is evident by the following metrices (Table 2) based on a total of 1049 subjects (training samples): the AUC increase from 0.6 (conventional ECG) to 0.7 (AI-enhanced ECG). Although the false positives (FP) increase by 144 samples, namely from 76 samples (conventional ECG) to 220 samples (AI-enhanced ECG), nevertheless, the true positives (TP) increase by 264 samples, namely from 236 samples (conventional ECG) to 500 samples (AI-enhanced ECG). Thus, compared with conventional ECG, the AI-enhanced ECG algorithm is able to identify an additional 264 subjects who were in need of clinical intervention and treatment.

4. Discussion

The major discovery of the present study is that our AI-enhanced ECG approach is able to improve the detection of CAD, and that this AI algorithm has a performance comparable to MPS-Thallium scanning. We have provided two examples to support the good performance of our AI-algorithm. The first example is a 61-year-old male patient who has a normal ECG and a negative result from a Thallium scan. Remarkably, our AI-enhanced ECG algorithm predicts the probability of CAD to be 0.75 (range from 0 to 1, threshold = 0.5). This is consistent with the invasive CAG result for this patient, which showed a significant infarction affecting the coronary arteries of this subject (Fig. 4A). Another example is a 60-year-old male non-CAD patient, who also has a normal ECG and a negative Thallium scan. His CAG revealed normal coronary arteries. Notably, the AI-algorithm predicts a very low probability of CAD, namely 0.27, for this subject (Fig. 4B). A graphic summary is presented in Fig. 4C.

Several findings can be pointed out. **Firstly**, our AI-enhanced ECG algorithm is able to act as an effective screening method when detecting CAD. For all subjects within the training (n = 5376) and validation (n = 7163) cohorts, the AUC is 0.84 and 0.91, respectively. In the subjects with normal ECGs, the AUC is 0.87 and 0.90 in the training (n = 2066) and validation (n = 4912) cohorts, respectively. **Secondly**, novel ECG features are able to be pinpointed by the XGBoost model. Interestingly, most of the top ranked features are associated with the slopes and amplitude differences between peaks. Notably, many features involve the T wave, indicating a key role for calcium reuptake and repolarization of the ventricular membranes. **Thirdly**, differences

Table 2
Comparison of the performance of conventional ECG, AI-enhanced ECG, and MPS-Thallium scan in detection of CAD.

Cohort	Sensitivity	Specificity	PPV	NPV	Accuracy	AUC	TP	FP	TN	FN
A. Conventional ECG										
Training (n = 1049)	**0.37**	**0.82**	**0.76**	**0.46**	**0.55**	**0.6**	**236**	**76**	**341**	**396**
Validation (n = 528)	**0.36**	**0.64**	**0.66**	**0.34**	**0.46**	**0.5**	**126**	**65**	**116**	**221**
B. AI-enhanced ECG algorithm (XGBoost)										
Training (n = 1049)	**0.79**	**0.47**	**0.69**	**0.6**	**0.66**	**0.7**	**500**	**220**	**197**	**132**
Validation (n = 528)	**0.83**	**0.2**	**0.67**	**0.38**	**0.61**	**0.57**	**288**	**145**	**36**	**59**
C. MPS-thallium scan										
Training (n = 1049)	**0.84**	**0.33**	**0.66**	**0.58**	**0.64**	**0.59**	**533**	**280**	**137**	**99**
Validation (n = 528)	**0.89**	**0.34**	**0.72**	**0.63**	**0.7**	**0.62**	**310**	**119**	**62**	**37**

PPV, positive predictive value; NPV, negative predictive value; AUC, area under curve; TP, true positive; FP, false positive; TN, true negative; FN, false negative.

between the sexes are highlighted by our findings and these affect the ranking of features tremendously. Accordingly, different prediction models need to be applied to males and females. **Lastly**, the performance of our AI-algorithm when detecting CAD is comparable to that of MPS-Thallium scanning, which is a nuclear medicine test. Thus, our AI-enhanced ECG approach provides an alternative to a nuclear isotope approach.

4.1. Sex differences and the AI-enhanced ECG approach

The distribution and kinetics of cardiac ion channels, as well as the effects of sex hormones on these channels, result in sex differences in the electric properties of cardiomyocytes, which in turn results in there being different ECG characteristics for the two sexes. This has potential implications in a clinical situation [26]. In males, the sex hormone androgen appears to shorten the QTc. This is in contrast with the longer QTc values observed in females; this effect is likely to be caused by a longer ST segment and a delayed start of the T wave [27]. Previously Lyle et al. applied the Symmetric Projection Attractor Reconstruction method to analyze the normal sinus rhythm of ECG signals as a two-dimensional image. Their study revealed a number of subtle differences, including some related to sex, others affecting ECG signals and yet others affecting ECG patterns. These are largely unrecognizable by human clinicians but seem to be able to be differentiated using an AI approach [21].

4.2. ECG features in CAD detection

Exercise-induced ST-segment depression or elevation predicts the presence of coronary artery stenosis. However, exercise-induced ST-segment elevation may also result from coronary artery spamming [28]. On the other hand, resting ECG with a de Winter pattern or a hyperacute T wave signifies the occlusion of coronary artery in only 2 % of CAD patients [29]. Other features of resting ECGs that indicate ischemic myocardium are T wave alterations and a giant R wave pattern [30,31]. Our findings reveal that many of the top features identified by our AI approach are related to the amplitudes of the R wave and T wave, and these probably reflect intracellular calcium release and reuptake by the sarcoplasmic reticulum. The top ranked features selected by our AI algorithm not only identify subtle alterations in ECG signals and patterns, but also help delineate the presence of an abnormal/damaged calcium cycle in the myocardium [32]. Interestingly, among the top fifteen features (Table S1), many are frequently associated with the long axis of the heart, namely leads I, II, aVL and aVF, which suggests that LAD stenosis may be prevalent in these cohorts. Additionally, leads V5 and V6 are often associated with the various top features and this may also reflect the prevalence of stenosis in the LAD or the LCX, which supply blood to the left ventricle.

4.3. Limitation and perspective

Additional efforts are needed to address several limitations of the present study. Firstly, it utilizes a combination of multiple ECG features to predict CAD, and this will present a new challenge for clinicians who are accustomed to analyzing ECG data using traditional parameters. Secondly, the electrophysiological implications of the individual ECG features remain unclear and needs further in-depth research. Thirdly, the long-term predictive outcomes of this study require further investigation. Fourthly, this is a cross-sectional study conducted on a single ethnic population. Although an external validation cohort was included, further validation of our findings on a larger scale and across ethnically diverse cohorts is necessary. Finally, according to our national regulations, this type of diagnostic assistant tool is classified as a Class II medical device. As such, it must be monitored by regulatory authorities or used under the supervision of an Institutional Review Board within medical institutions. Accordingly, it will be challenging to make the web application publicly available at the present time.

Furthermore, recently McKeen et al. [33] developed an ECG-Foundation Model (ECG-FM); this model adopts a transformer-based architecture. One of our future areas of interest will be to use ECG-FM as a pretrained model and fine tune a downstream task stream that will be able to classify the presence or absence of significant coronary artery stenosis. For an explainable model perspective, inspired by Budhkar et al. [34], the ECG feature created in this study may be applicable as a graph model, thus allowing the exploration of the connections between different leads, various features and stenosis of the coronary arteries.

5. Conclusions

In conclusion, our study reveals that AI-enhanced ECG algorithms are able to provide a noninvasive method that upgrades the current ECG approach in order to identify a subset of high-risk patients with stable chest pain. The new ECG features pinpointed using a 12-lead ECG and our AI algorithm should be able to serve as digital biomarkers for CAD. Importantly, at the personal level, each individual has a personal feature ranking list calculated by the SHAP framework. The introduction of the SHAP values will help clinicians understand the importance of the different ECG features of each patient thereby enabling a more precise diagnosis and a more targeted treatment, both of which will advance personalized medicine in relation to CAD.

CRediT authorship contribution statement

Chun-Tai Mao: Writing – original draft, Investigation, Funding acquisition, Data curation, Conceptualization. **Tzu-Pei Su:** Writing – original draft, Formal analysis, Data curation. **Chun-Hung Chen:** Writing – original draft, Methodology, Formal analysis, Data curation. **Yi-Ju Chou:** Writing – original draft, Visualization, Methodology, Data curation. **Ning-I Yang:** Writing – original draft, Investigation, Funding acquisition, Data curation, Conceptualization. **Chi-Chun Lai:** Writing – original draft, Supervision, Methodology, Funding acquisition, Data curation. **Chien-Tzung Chen:** Writing – original draft, Supervision, Investigation, Funding acquisition, Conceptualization. **Chi-Hsiao Yeh:**

Writing – review & editing, Writing – original draft, Validation, Data curation, Conceptualization. **Tsung-Hsien Tsai:** Validation, Methodology, Formal analysis, Data curation. **Huey-Kang Sytwu:** Writing – original draft, Validation, Supervision, Investigation, Funding acquisition. **Ting-Fen Tsai:** Writing – review & editing, Writing – original draft, Validation, Supervision, Investigation, Conceptualization.

Declaration of Competing Interest

YJC, CTM, TPS, NIY, CCL, CTC, HKS, and SFT do not have competing interests to disclose. CHY, THT, CHC, and TFT are inventors on the Taiwan patent I768624.

Acknowledgments

This research was funded by grants from the Ministry of Health and Welfare (Smart Healthcare for Obesity Therapeutics; PD-109-GP-02, MG-110-GP-03 and MG-111-GP-03 to HKS) and Chang Gung Memorial Hospital (CRRPG2H0191–0193 to CTM; CRRPG2H0181–0183 to NIY, CRRPG2H0171–0173 to CHY; CORPG2K0011–0013 to CCL). We acknowledge the participant recruitment and sample preservation carried out as part of the Northeastern Taiwan Community Medicine Research Cohort Study.

Appendix A. Supporting information

Supplementary data associated with this article can be found in the online version at doi:10.1016/j.csbj.2024.12.032.

References

[1] Perez MV, et al. Large-scale assessment of a smartwatch to identify atrial fibrillation. N Engl J Med 2019;381(20):1909–17.
[2] Adedinsewo D, et al. Artificial intelligence-enabled ECG algorithm to identify patients with left ventricular systolic dysfunction presenting to the emergency department with dyspnea. Circ Arrhythm Electro 2020;13(8):e008437.
[3] Attia ZI, et al. Screening for cardiac contractile dysfunction using an artificial intelligence-enabled electrocardiogram. Nat Med 2019;25(1):70–4.
[4] Cohen-Shelly M, et al. Electrocardiogram screening for aortic valve stenosis using artificial intelligence. Eur Heart J 2021.
[5] Galloway CD, et al. Development and validation of a deep-learning model to screen for hyperkalemia from the electrocardiogram. JAMA Cardiol 2019;4(5):428–36.
[6] Attia ZI, et al. Noninvasive assessment of dofetilide plasma concentration using a deep learning (neural network) analysis of the surface electrocardiogram: A proof of concept study. PLoS One 2018;13(8):e0201059.
[7] Siontis KC, et al. Artificial intelligence-enhanced electrocardiography in cardiovascular disease management. Nat Rev Cardiol 2021;18(7):465–78.
[8] Doorey AJ. Normal ECG in Patients With Severe Coronary Artery Disease. JAMA 1997;277(12):956. 956.
[9] Topaz O, et al. Isolated significant left main coronary artery stenosis: angiographic, hemodynamic, and clinical findings in 16 patients. Am Heart J 1991;122(5):1308–14.
[10] Christian TF, et al. Exercise tomographic thallium-201 imaging in patients with severe coronary artery disease and normal electrocardiograms. Ann Intern Med 1994;121(11):825–32.
[11] van Klei WA, et al. The value of routine preoperative electrocardiography in predicting myocardial infarction after noncardiac surgery. Ann Surg 2007;246(2):165–70.
[12] Meller B, et al. Accelerated diagnostic protocol using high-sensitivity cardiac troponin T in acute chest pain patients. Int J Cardiol 2015;184:208–15.
[13] Anderson KP. Artificial intelligence-augmented ECG assessment: The promise and the challenge. J Cardiovasc Electro 2019;30(5):675–8.
[14] Attia IZ, et al. External validation of a deep learning electrocardiogram algorithm to detect ventricular dysfunction. Int J Cardiol 2021;329:130–5.
[15] Attia ZI, et al. Artificial Intelligence ECG to Detect Left Ventricular Dysfunction in COVID-19: A Case Series. Mayo Clin Proc 2020;95(11):2464–6.
[16] Attia ZI, et al. Prospective validation of a deep learning electrocardiogram algorithm for the detection of left ventricular systolic dysfunction. J Cardiovasc Electro 2019;30(5):668–74.
[17] Attia ZI, et al. An artificial intelligence-enabled ECG algorithm for the identification of patients with atrial fibrillation during sinus rhythm: a retrospective analysis of outcome prediction. Lancet 2019;394(10201):861–7.
[18] Huang PS, et al. An artificial intelligence-enabled ECG algorithm for the prediction and localization of angiography-proven coronary artery disease. Biomedicines 2022;10(2).
[19] Attia ZI, et al. Age and sex estimation using artificial intelligence from standard 12-Lead ECGs. Cir Arrhythm Electro 2019;12(9):e007284.
[20] Macfarlane PW. The influence of age and sex on the electrocardiogram. Adv Exp Med Biol 2018;1065:93–106.
[21] Maioli V, Clementi L, Santambrogio MD. Sex differences in the ECG interpretation: a functional data analysis perspective. *2021 IEEE 6th Int Forum Res Technol Soc Ind (RTSI)* 2021.
[22] Malik M, et al. QT/RR curvatures in healthy subjects: sex differences and covariates. Am J Physiol Heart Circ Physiol 2013;305(12):H1798–806.
[23] Dzaye O, et al. Modeling the recommended age for initiating coronary artery calcium testing among at-risk young adults. J Am Coll Cardiol 2021;78(16):1573–83.
[24] Huang Y, et al. Sexual differences in genetic predisposition of coronary artery disease. Cir Genom Precis Med 2021;14(1):e003147.
[25] Underwood SR, et al. Myocardial perfusion scintigraphy: the evidence. Eur J Nucl Med Mol Imaging 2004;31(2):261–91.
[26] Amuthan R, Curtis AB. Sex-specific considerations in drug and device therapy of cardiac arrhythmias: JACC Focus Seminar 6/7. J Am Coll Cardiol 2022;79(15):1519–29.
[27] Lehmann MH, Yang H. Sexual dimorphism in the electrocardiographic dynamics of human ventricular repolarization. Circulation 2001;104(1):32–8.
[28] Waters DD, et al. Clinical and angiographic correlates of exercise-induced ST-segment elevation. Increased detection with multiple ECG leads. Circulation 1980;61(2):286–96.
[29] Goebel M, et al. A new ST-segment elevation myocardial infarction equivalent pattern? Prominent T wave and J-point depression in the precordial leads associated with ST-segment elevation in lead aVr. Am J Emerg Med 2014;32(3):287. e5-287.e8.
[30] Ortega-Carnicer J. Giant R wave, convex ST-segment elevation, and negative T wave during exercise treadmill test. J Electro 2004;37(3):231–6.
[31] Verrier RL, Nearing BD. Electrophysiologic basis for T wave alternans as an index of vulnerability to ventricular fibrillation. J Cardiovasc Electro 1994;5(5):445–61.
[32] Slezak J, et al. Hibernating myocardium: pathophysiology, diagnosis, and treatmentThis article is one of a selection of papers from the NATO Advanced Research Workshop on Translational Knowledge for Heart Health (published in part 2 of a 2-part Special Issue). Can J Physiol Pharm 2009;87(4):252–65.
[33] McKeen, K., et al., ECG-FM: An open electrocardiogram foundation model. arXiv 2024. arXiv:2408.05178v1. doi.org: 10.48550/arXiv.2408.05178.
[34] Budhkar A, et al. xSiGra: explainable model for single-cell spatial data elucidation. Brief Bioinform 2024;25(5):bbae388.